Research on Chemical Intermediates (2021) 47:4985–5005
https://doi.org/10.1007/s11164-021-04576-7

Synthesis, structure characterization and quantum chemical study on relationship between structure and antioxidant properties of novel Schiff bases bearing (thio)/carbohydrazones

Halit Muğlu, et al. ***[full author details at the end of the article]***

Received: 23 June 2021 / Accepted: 18 August 2021 / Published online: 29 August 2021

Abstract

A series of novel isatin-based Schiff base derivatives, namely *β*-isatin aldehyde-*N,N′*-(thio)/carbohydrazone derivatives (**1–8**), have been synthesized. All of the compounds were purified, and IR, ^{1}H NMR and ^{13}C NMR spectroscopic methods and elemental analysis were used to characterize the compounds. Moreover, the in vitro antioxidant activity of the compounds was evaluated by 1,1-diphenyl-2-picrylhydrazyl (DPPH) free radical scavenging method and compared with standard natural antioxidant, gallic acid. Experimental data were supported by density functional theory (DFT) calculations. B3LYP hybrid functional with 6–311 + + g(2d,2p) basis set was used to calculate ground-state geometries, FMO energies and related chemical reactivity parameters of the compounds. In addition to the structural and spectral analysis calculations of the compounds, NBO, QTAIM, NCI, Fukui and DOS analyses were also performed at the same level of theory, and the data were used to determine the effects of conformational and electronic properties of substitute groups in the reactive regions of the compounds on the reaction with DPPH and to analyze the antioxidant behavior of the compounds.

Graphic abstract

New Schiff bases bearing (thio)/carbohydrazone and isatin were synthesized. Structures of synthesized compounds were elucidated using spectroscopic techniques. Antioxidant activities of the compounds were measured by DPPH method. FMO

energies, NBO, QTAIM, NCI, Fukui and DOS analyses were used to examine the relationship between the electronic properties and antioxidant activity.

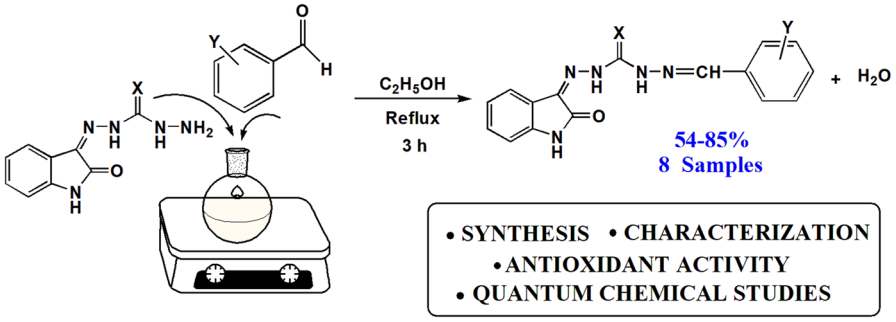

Keywords Isatin · Schiff bases · Antioxidant activity · Spectroscopic techniques · Quantum chemical studies

Introduction

Isatin is an endogenous compound identified in the human body [1]. Isatins (indole-2,3-diones) are a significant class of heterocyclic compounds in chemistry. Isatin derivatives have shown a variety of biological and medicinal activities, such as antioxidant [2, 3], antibacterial [4–6], antimicrobial [7, 8], antiviral [9], anti-HIV [10], anticonvulsant [11], antitubercular [12] and anticancer [13–15].

Schiff bases compounds, including the azomethine group (–CH=N–), have a wide range of chemical, pharmacological and biological properties such as magnetic properties [16], anticancer [17], enzyme inhibitor [18], photocatalyst [19], anti-inflammatory [20], antimicrobial [21], antioxidant [22–24], cytotoxic activity [25] and antibacterial [26].

In the literature, there are several studies on the application of thioureas and urea (–NH–(C=X)–NH–) as potential applications in organic, materials, organocatalysts as well as medicinal chemistry [27, 28].

Antioxidants are known as compounds that prevent organism and cell damage due to oxidative stress [29]. Schiff bases and complexes have been the subject of research, with their important properties such as binding redox systems in reversible oxygen in biological systems and preventing or reducing DNA oxidation [30, 31]. It has been shown in recent years that various isatin derivatives exhibit antioxidant properties as well as many biochemical properties [32–34]. Isatin shows 72.8 mg/mL antioxidant activity with EC_{50} [35]. Besides, another study reported that *β*-isatin-*N,N'*-thiocarbohydrazone derivatives exhibit antimicrobial and antioxidant activity [36]. A recent study on thymol and carvacrol Schiff base derivatives with a concentration of 5 µg/mL reported that antioxidant activity was observed with 60–90% inhibition [37].

In this context, isatin-based Schiff bases are significant not only in possessing biological activities, but also in pharmacological properties. In this study, novel isatin-based Schiff base derivatives were obtained by reaction of (thio)/carbohydrazides with various aromatic aldehydes. The structures of all synthesized compounds were confirmed by using IR, ^{1}H NMR and ^{13}C NMR spectroscopic techniques and elemental analysis. The experimental results were supported by DFT calculations. The electronic properties of the compounds were examined, and how the substituents affect the electronic properties of the compounds were analyzed by natural bond orbital (NBO), quantum theory atom in molecule (QTAIM), non-covalent interaction (NCI), Fukui and density-of-state (DOS) calculations. Moreover, the intramolecular interactions of the substituents that play an active role in the DPPH reaction and the effects of these interactions on the reactivities of the compounds were also investigated. Furthermore, the in vitro antioxidant activities of the products were tested by the free radical scavenging method because antioxidants can trap free radicals and diminish damage effect in our bodies.

Experimental section

Measurement and reagents

All chemical reagents and solvents were purchased from Carlo Erba, Riedel-deHaën, Acrõs Organics, Aldrich and Merck Chemical Company and were used without further purification. The IR spectra were recorded on a Bruker Vertex 80v spectrophotometer. ^{1}H NMR and ^{13}C NMR spectra were determined in dimethyl sulfoxide-d_6 (DMSO-d_6) on a Bruker Avance DPX-400 (400 MHz) spectrophotometer using TMS as the internal standard. Melting points were measured with a Stuart SMP 30 electrothermal apparatus and are uncorrected. Elemental analyses were performed on a EuroVector EA3000 elemental analyzer with the VTF-900 high-temperature pyrolysis furnace. UV–Vis spectra and absorption data obtain a Pharmaspec 1700 UV–visible spectrophotometer.

Synthesis of novel isatin-based Schiff base derivatives

A mixture of indoline-2,3-dione (isatin) (5.0 mmol) and thiocarbohydrazide or carbohydrazide (5.0 mmol) in ethanol (20 mL) and two drops of hydrochloric acid was refluxed for 3–5 h. The reaction mixture was cooled, and the precipitate formed was filtered and washed with ethanol (96%) to give isatin-β-(thio)/carbohydrazone. A mixture of isatin-β-(thio)/carbohydrazone (2.0 mmol), aromatic aldehydes (2.0 mmol) and two drops of hydrochloric acid in ethanol (20 mL) was refluxed for 3 h. The color precipitate formed was filtered and washed with ethanol (96%) to give a product. The reaction route is given in Scheme 1. They were obtained with slight changes according to an earlier procedure [36].

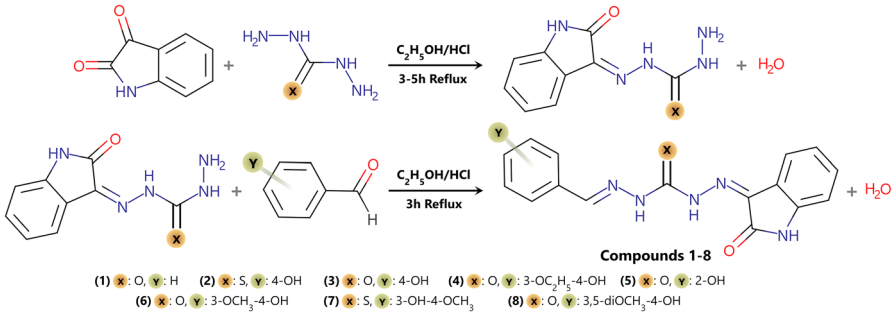

Scheme 1 Synthetic route for novel isatin-based Schiff bases (**1–8**)

Antioxidant activity measurements by DPPH method

The DPPH method, one of the antioxidant activity assays, is used to study the radical scavenging activities of molecules based on the hydrogen atom transfer reaction and the hydrogen loss capacity/ability of the compounds. Antioxidant activity determinations of compounds (**1**–**8**) synthesized using DPPH free radical cleaning method were performed. For this purpose, known method implementation was used with minor changes [38, 39]. Stock solutions of synthesized compounds were prepared by weighing 250 µM in DMSO. Three milliliters of 250 µM DPPH solution and different volumes (10–200 µL) of stock solutions were completed to a total of 6 mL with sufficient ethanol. Compound concentrations in the range of 0.5–10 µM were obtained by adding to the previously prepared DPPH solution. The prepared mixes were allowed to stand for 30 min at room temperature in a dark room and then read against a sample without sample at 517 nm. Antioxidant activity was expressed as a percentage of inhibition and was calculated using the following equation [40]:

$$(\%)\text{inhibition} = [(\text{A0} - \text{A1})/\text{A0} \times 100].$$

Here, A_0 is used as the absorbance of the control (empty, no compound) and the absorbance of the compound A_1. Then, IC_{50} (mg/mL) values expressing the amount of antioxidants needed to reduce the initial DPPH concentration by 50% were used to measure antioxidant activity [41].

Computational procedure

All calculations were performed with the Gaussian 09 software [42] using the Kohn–Sham density functional theory (KS-DFT) [43, 44], using the B3LYP functional with 6–311 + + G(2d,2p) basis set. There are no imaginary frequencies in the IR calculations of the optimized compounds, and their energies are the global minimum points corresponding to the lowest energy on the potential energy surfaces (PESs). For NMR calculations, the compounds were re-optimized in the DMSO phase, and gauge-independent atomic orbital (GIAO) method was used for calculations of ^{1}H and ^{13}C NMR. The conductor-like polarizable continuum model (CPCM) was used to model solvation effects. By subtracting the TMS shielding

(31.8149 ppm for ^{1}H NMR and 183.7737 ppm for ^{13}C NMR), relative chemical shift values were calculated. To calculate global chemical reactivity parameters such as chemical hardness and electronegativity, the HOMO–LUMO energy eigenvalues were used.

Using natural bond orbitals (NBOs) population analysis [45–50], charging distribution on the individual atoms of the compounds was evaluated. Moreover, Bader's quantum theory of atoms in molecules (QTAIM) [51–54] was also used to analyze the electron density distributions in the compounds. QTAIM analysis was also performed to determine the intramolecular interactions and to determine the ring-critical points (RCPs) of the charge density distribution and the bond-critical points (BCPs) of the bonding atoms. In addition, calculations of the electron density (ρ), potential energy density (V), delocalization index (DI), bond path length (BPL) and bond length (L) of the active phenolic O–H bonds were also determined and associated with the antioxidant properties of the compounds. Moreover, NCI and Fukui calculations were also used to analyze the electronic properties of intramolecular interactions and electrophilic attack sites.

Results and discussion

Physical properties

The names, melting points, yields and basic analysis data of the synthesized compounds are summarized in Tables 1 and 2. Figure 1 is used in the interpretation of both spectral and electronic data in the following sections.

Vibrational frequencies

In the FTIR spectra, the signal of the aldehyde group (–CHO, two bands) of the starting material was not observed at 2750–2680 cm^{-1}. Moreover, the symmetric and asymmetric stretching bands of the amino group ($–NH_2$) did not show at 3520–3250 cm^{-1}. Instead, new –C=N stretching vibrations of imine group were observed at 1620–1510 cm^{-1}. These results indicated a successful reaction, as expected. For compound **2**, the –NH vibration was observed at 3147 cm^{-1} as shown in Figure S2. The O–H signal of phenolic region was observed at 3232 cm^{-1}. The C=O signal of isatin ring was observed at 1696 cm^{-1}. The –C=N stretching vibration was observed at 1574 cm^{-1}; the C=S signal of thiocarbohydrazide region was observed at 1464 cm^{-1}; the –C–N stretching vibration was observed at 1249 cm^{-1}; and the –C–O signal of aryl ring was observed at 1163 cm^{-1}. These frequency values of the compounds were in agreement with those of similar compounds [4, 9, 55]. IR vibrations for the synthesized compounds are presented in Table 3. For the synthesized compounds (**1–8**), the –NH vibrations were observed at 3245–3143 cm^{-1}, aromatic proton vibrations were observed at 3114–3000 cm^{-1}, the –C=O signals of isatin region were observed at 1732–1696 cm^{-1}, the –C=N signals of isatin region were observed at 1595–1574 cm^{-1}, and the –C–N group absorptions were

Table 1 Physical data, melting points and yields for the compounds (**1**–**8**)

Comp.	Compounds name	− Y	Yield %	M. P. (°C)	Color	Solubility
1	1-Benzylidene-5-(2-oxoindoline-3-ylidene) carbohydrazone	H	62	272–273	Yellow	DMSO (+)
2	1-(4-Hydroxy-benzylidene)-5-(2-oxoindoline-3-ylidene) thiocarbohydrazone	4-OH (X:S)	73	259–260	Light Orange	DMSO (+)
3	1-(4-Hydroxy-benzylidene)-5-(2-oxoindoline-3-ylidene) carbohydrazone	4-OH	85	274–275	Yellow	DMSO (+)
4	1-(3-Etoxy-4-hydroxy-benzylidene)-5-(2-oxoindoline-3-ylidene) carbohydrazone	3-OC_2H_5-4-OH	55	268–269	Yellow	DMSO (+)
5	1-(2-Hydroxy-benzylidene)-5-(2-oxoindoline-3-ylidene) carbohydrazone	2-OH	54	259–260	Yellow	DMSO (+)
6	1-(4-Hydroxy-3-methoxy-benzylidene)-5-(2-oxoindoline-3-ylidene) carbohydrazone	3-OCH_3-4-OH	66	274–275	Yellow	DMSO (+)
7	1-(3-Hydroxy-4-methoxy-benzylidene)-5-(2-oxoindoline-3-ylidene) thiocarbohydrazone	3-OH-4-OCH_3 (X:S)	60	237–238	Light Orange	DMSO (+)
8	1-(4-Hydroxy-3,5-dimethoxy-benzylidene)-5-(2-oxoindoline-3-ylidene) carbohydrazone	3,5-diOCH_3-4-OH	62	271–272	Yellow	DMSO (+)

Table 2 Elemental analysis results of the compounds

Comp	Mol mass (g/mol)	Molecular formula	Calculated			Experimental		
			C%	H%	N%	(C) %	(H) %	(N) %
1	307.31	$C_{16}H_{13}N_5O_2$	62.53	4.26	22.79	62.35	4.21	22.65
2	339.38	$C_{16}H_{13}N_5O_2S$	56.63	3.86	20.64	56.48	3.82	20.72
3	323.31	$C_{16}H_{13}N_5O_3$	59.44	4.05	21.66	59.55	4.01	21.72
4	367.36	$C_{18}H_{17}N_5O_4$	58.85	4.66	19.06	58.78	4.59	19.13
5	323.21	$C_{16}H_{13}N_5O_3$	59.44	4.05	21.66	59.37	4.09	21.59
6	353.34	$C_{17}H_{15}N_5O_4$	57.79	4.28	19.82	57.68	4.23	19.76
7	369.40	$C_{17}H_{15}N_5O_3S$	55.27	4.09	18.96	55.36	4.04	18.88
8	383.36	$C_{18}H_{17}N_5O_5$	56.39	4.47	18.27	56.43	4.44	18.22

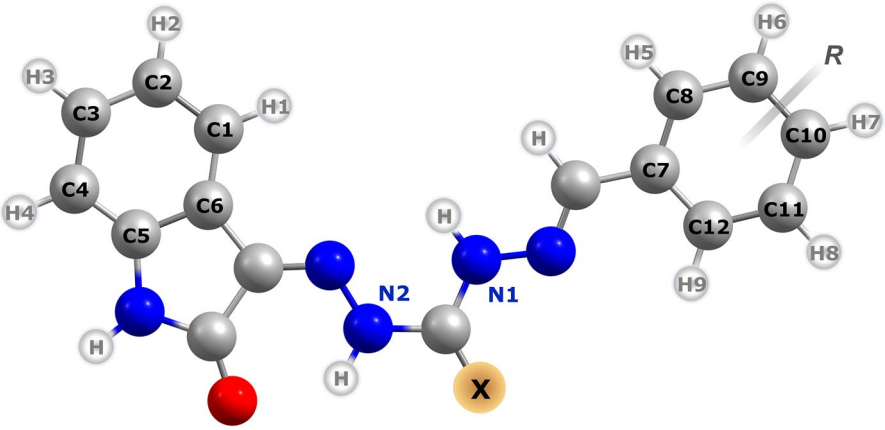

Fig. 1 Numbering of the atoms on the compounds

observed at 1270–1242 cm^{-1}. The OH signal of phenolic region was observed at 3474–3232 cm^{-1}, and the –C–O group vibrations were observed at 1163–1141 cm^{-1}. Except for compounds **2** and **7**, the –C=X signals of carbohydrazone region were observed at 1694–1656 cm^{-1}. All of the IR spectra of the compounds are given in supplementary material (Figures S1–S8).

^{1}H NMR interpretations

The ^{1}H NMR spectra of the synthesized compounds were detected in DMSO-d_6 solvent. For compound **2**, the aromatic proton signals of aryl ring (H5, H6, H8 and H9) were observed between 6.84 and 7.75 ppm (Fig. 2). H5 and H9 (2H) coupled to H6 and H8 proton and showed doublet peaks at 7.73–7.75 ppm. H6 and H8 (2H) coupled to H5 and H9 and observed doublet peaks at 6.84–6.86 ppm. H4 coupled to H3 and detected doublet peaks at 7.57–7.59 ppm. H3 coupled to H2 and H4 and

Table 3 IR vibration values for the synthesized compounds

Comp.	OH	–NH	Ar CH	C=X	C=O	C=N	C–N	C–O	Aliph CH
Experimental									
1	–	3188	3071	1656	1713	1574	1262	–	–
2	3232	3147	3000	1464	1696	1574	1249	1163	–
3	3336	3193	3080	1691	1731	1591	1264	1145	–
4	3395	3175	3079	1680	1731	1584	1248	1147	2973
5	3274	3143	3060	1694	1729	1595	1261	1137	–
6	3328	3175	3059	1683	1731	1593	1270	1141	2955
7	3474	3245	3114	1456	1696	1576	1250	1162	2947
8	3284	3194	3105	1676	1732	1586	1242	1161	2947
Calculated									
1	–	3646	3205–3163	1790	1749	1672	1258	–	–
2	3833	3647	3204–3161	1522	1749	1668	1196	1285	3024
3	3833	3646	3203–3160	1786	1749	1674	1258	1283	3022
4	3781	3646	3203–3186	1789	1748	1672	1259	1301	3016
5	–	3645	3204–3163	1785	1750	1666	1258	1307	3047
6	3783	3646	3203–3186	1789	1749	1673	1259	1302	3016
7	3791	3647	3212–3178	1521	1749	1665	1204	1298	3026
8	3769	3646	3203–3186	1786	1748	1669	1260	1267	3030

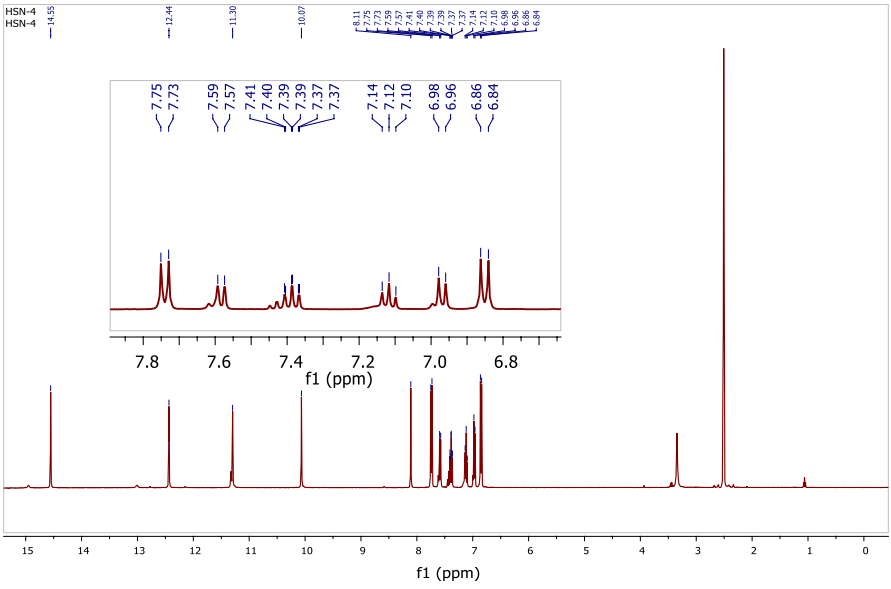

Fig. 2 ^{1}H NMR spectrum of compound **2**

detected multiplet peaks at 7.37–7.41 ppm. H2 coupled to H3 and H1 and detected triplet peaks at 7.10–7.14 ppm. H1 coupled to H2 and detected doublet peaks at 6.96–6.98 ppm. The hydroxyl group (–OH) proton signals were detected as a singlet at 10.07 ppm. The signal of imine (–CH=N) was observed as a singlet at 8.11 ppm. The proton signals of isatin and thiocarbohydrazone regions were observed from –NH, $–N^1H$ and $–N^2H$. These amino peaks were observed as a singlet at 14.55, 11.30 and 12.44 ppm, respectively. DMSO-d_6 and water in DMSO (HOD, H_2O) signals are shown around at 2.00, 2.50 (quintet) and 3.30 ppm (variable, based on the solvent and its concentration), respectively [56]. These data are consistent with the values of earlier reported similar compounds [4, 9, 24, 55, 57, 58]. The chemical shifts of all synthesized compounds are shown in Table 4, and all of ^{1}H NMR spectra of the compounds are given in supplementary material (Figures S9–S15).

^{13}C NMR interpretations

The ^{13}C NMR spectra of all compounds were obtained in DMSO-d_6 a solvent. The ^{13}C NMR spectrum of compound **2** showed 16 different resonances in good agreement with the proposed structure as shown in Fig. 3. In compound **2**, –C=S signal of thiocarbohydrazide region was detected at 175.4 ppm. The characteristic –CH=N (imin) peak was observed at 145.4 ppm. The carbonyl atom (–C=O) of isatin region was observed at 163.3 ppm. The –C=N vibrations of isatin ring were observed at 137.9 ppm. The aromatic carbons (C7–C12) were also observed at 125.0, 129.9, 116.3, 160.7, 116.3 and 129.9 ppm, respectively. The resonance of the C10 carbon atom shifted down-field due to the presence of electron-withdrawing group of –OH. The aromatic carbons (C1–C6) of isatin region were also observed at 121.2, 120.6, 131.7, 111.6, 142.6 and 123.0 ppm, respectively. These spectroscopic data are consistent with the values of previously reported similar compounds and the literature [4, 9, 55]. Also, the chemical shifts of all products are presented in Table 5, and all of ^{13}C NMR spectra of the compounds are given in supplementary material (Figures S16–S22).

Evaluation of antioxidant activity assays

For synthesized compounds (**1**–**8**), antioxidant activity assessment performed by DPPH radical removal method is given in Fig. 4 in terms of inhibition percentages calculated against concentration using gallic acid as standard.

In this study, antioxidant inhibition percentages of the compounds showed a regular increase in direct proportion to the increase in concentration. Compounds **2** and **4** showed the highest inhibition rates among other compounds, although they were low compared to standard antioxidant. Compound **6** showed a higher percentage inhibition in the concentration ranges of 0.5–2.5 μM, but showed a lower increase in concentrations of 5–10 μM and showed a stable state in percent inhibition.

In addition, IC_{50} values were calculated to determine and evaluate the antioxidant activities of gallic acid and compounds, and the data are summarized in Table 6. Considering the IC_{50} values of the compounds, it is seen that the compounds have

Table 4 ^{1}H NMR (δ, ppm, in DMSO–d_6) values of synthesized compounds

Comp	Isatin NH	N^2H–N	=N–N^1H	CH=N	–Ar H, isatin H	–OH	–CH_3/OCH_3
Experimental							
1	13.77	11.39	11.24	8.01	7.84–7.82 (1H, d, ArH7) 7.58–7.56 (1H, d, H4) 7.47–7.45 (2H, m, ArH5,H9) 7.41–7.36 (2H, m, ArH6,H8) 7.15–7.09 (2H, m, H2,H3) 6.98–6.95 (1H, dd, H1)	–	–
2	14.55	12.44	11.30	8.11	7.75–7.73 (2H, d, ArH5,H9) 6.86–6.84 (2H, d, ArH6,H8) 7.59–7.57 (1H, d, H4) 7.41–7.37 (1H, m, H3) 7.14–7.10 (1H, t, H2) 6.98–6.96 (1H, d, H1)	10.07	–
3	13.69	11.25	11.17	7.90	7.66–7.64 (2H, d, ArH5,H9) 6.84–6.82 (2H, d, ArH6,H8) 7.58–7.55 (1H, t, H4) 7.42–7.34 (1H, td, H3) 7.16–7.08 (1H, td, H2) 6.99–6.95 (1H, t, H1)	9.92	–
4	13.73	11.24	11.19	9.41	7.86 (1H, s, ArH5) 7.58–7.54 (1H, d, ArH9) 6.83–6.81 (1H, d, ArH8) 7.41–7.34 (1H, m, H4) 7.15–7.06 (2H, m, H2,H3) 6.99–6.96 (1H, dd, H1)	11.16	4.21–4.16 (2H, q, –CH_2) 1.44–1.40 (3H, t, –CH_3)
5	13.72	11.25	11.20	8.36	7.58–7.56 (1H, d, ArH9) 7.42–7.40 (1H, m, H4) 7.38–7.34 (1H, m, H7) 7.25–7.23(1H, m, H8) 6.92–6.86 (1H, m, H6) 7.15–7.09 (2H, m, H2,H3) 6.99–6.95(1H, dd, H1)	10.02	–
6	13.81	11.80	11.28	8.21	7.61–7.56 (2H, d, ArH9,H8) 7.41–7.38 (1H, t, H4) 7.22 (1H, s, ArH5) 7.15–7.07 (1H, m, H3) 6.99–6.92 (1H, m, H1,H2)	11.03	3.18 (3H, s, –OCH_3)
7	14.54	12.43	11.29	8.07	7.59–7.58 (1H, d, ArH6) 7.36–7.35 (1H, d, ArH9) 7.03 (1H, s, ArH5) 7.30–7.27 (1H, dd, H4) 7.14–7.10 (1H, t, H3) 7.01–6.96(1H, t, H2) 7.41–7.37 (1H, dt, H1)	9.11	3.85 (3H, s, –OCH_3)

Table 4 (continued)

Comp	Isatin NH	N^2H–N	=N–N^1H	CH=N	–Ar H, isatin H	–OH	–CH_3/OCH_3
8	13.75	11.27	11.19	7.87	7.16 (2H, d, ArH5,H9) 7.59–7.54 (1H, dd, H4) 7.40–7.33 (1H, t, H3) 7.12–7.08 (1H, t, H2) 6.99–6.94 (1H, dd, H1)	8.81	3.87 (6H, s, –CH_3)
Calculated							
1	7.46	12.44	9.95	8.38	7.86, 8.63 (H5, H9) 7.86–7.93 (H6, H8) 7.87 (H7), 7.31 (H4) 7.73 (H3), 7.55 (H2) 8.06 (H1)	–	–
2	7.46	13.21	10.92	8.52	7.81, 8.55 (H5, H9) 7.29–7.22 (H6, H8) 7.29 (H4), 7.73 (H3) 7.55 (H2), 8.09 (H1)	5.34	–
3	7.46	12.38	9.81	8.29	8.46, 7.75 (H5, H9) 7.29, 7.20 (H6, H8) 7.29 (H4), 7.70 (H3) 7.55 (H2), 8.06 (H1)	5.25	–
4	7.50	12.30	9.80	8.35	7.23, 8.12 (H5, H9) 7.34 (H8), 7.31 (H4) 7.51–7.79 (H2, H3) 8.11 (H1)	6.22	4.30 (–CH_2) 1.61–1.48 (–CH_3)
5	7.43	12.45	9.86	8.55	7.73 (H5) 7.27, 7.47 (H6, H8) 7.79 (H7), 7.29 (H4) 7.73 (H3), 7.55 (H2) 8.05 (H1)	11.74	–
6	7.49	12.35	9.84	8.31	7.25, 8.12 (H5, H9) 7.32 (H8), 7.30 (H4) 7.74 (H3), 7.53 (H2) 8.12 (H1)	6.21	4.37–4.01 (–CH_3)
7	7.48	13.19	10.94	8.46	7.24 (H6), 8.11 (H1) 8.09 (H9), 7.24 (H4) 7.73 (H3), 7.42 (H5) 7.54 (H2)	5.76	4.43–3.99 (–OCH_3)
8	7.45	12.43	9.84	8.19	7.30 (H4), 7.69 (H3) 7.13, 7.78 (H5, H9) 7.56 (H2), 8.07 (H1)	8.74	3.80 (6H, s, –CH_3)

an increased antioxidant activity in the order of 2 > 4 > 8 > 6 > 7 > 3 > 1 > 5. Benzaldehyde-derived compounds containing *m*-substituted groups showed higher antioxidant activity.

The presence of electron providing methoxy and ethoxy groups in the compounds containing phenolic structure (**4**, **6**, **7**, **8**) contributed to the increase in the antioxidant activity of the compound. The isatin structure used without substitution showed higher antioxidant activity than 5-chloro isatin molecule. This result confirms that the lipophilicity of the molecule increases as a result of the presence of

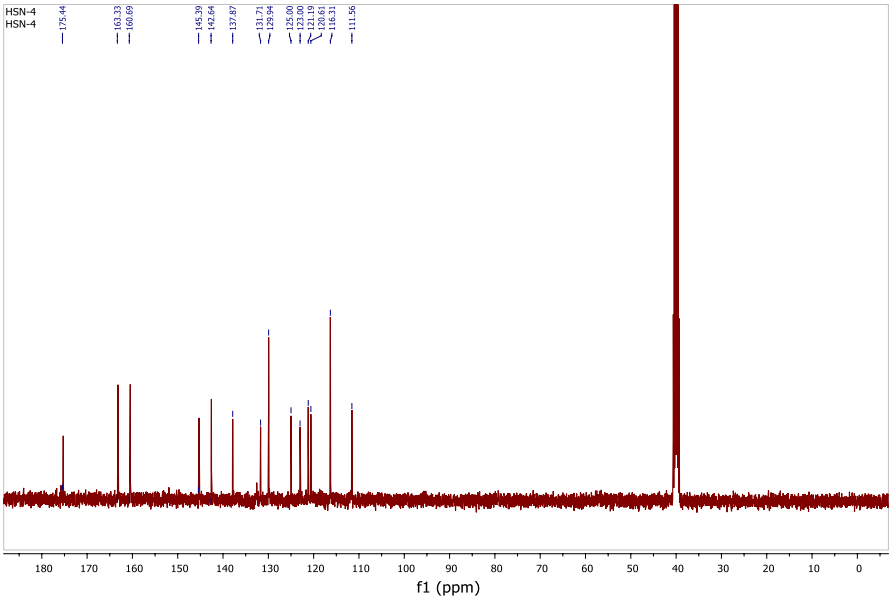

Fig. 3 ^{13}C NMR spectrum of compound **2**

an electronegative atom such as chloride on the aromatic ring and causes a lower observation of antioxidant activity [22]. While compound **2** with the structure of *p*-hydroxybenzaldehyde has the highest antioxidant activity, compound **3** containing the *p*-hydroxybenzaldehyde structure was found to have much lower antioxidant activity. This result can be explained by the presence of thio group in the compounds, showing better antioxidant properties [58].

Theoretical analysis

The effects of the substituents and their positions on determining the electronic properties of the compounds and also their antioxidant properties were studied theoretically. Compound **1**, which did not contain a functional substituent on the aryl group, was chosen as the reference compound, and thus, the effects of the substituents were analyzed comparatively. Comparison of the electronic properties of the position and structure of the substituents of the compounds was made between compounds **1** and **2**; compounds **2** and **3**; compounds **3** and **4**; compounds **4** and **6**; and compounds **6** and **8**. Thus, a comparative analysis of the effects of each functional group was performed.

Some calculated electronic parameters of the compounds are given in Table 7. The HOMO–LUMO gap represents the region where the most likely excitations can occur, that is, the gap in the binding energy spectrum is called the LUMO–HOMO gap, and the smaller the HOMO–LUMO energy gap ΔE, the easier it is for excitation. Non-substituted compound **1** had the highest ΔE and the lowest antioxidant

Table 5 ^{13}C NMR data of compounds **1–8** (δ/ppm)

	Ist C=O	Ist C=N	C=X	CH=N	C1	C2	C3	C4	C5	C6	C7	C8	C9	C10	C11	C12	Subs
Experimental																	
1	163.3	134.7	163.1	151.8	120.7	120.3	131.9	111.4	142.2	122.9	131.2	129.3	127.3	130.4	127.3	129.3	–
2	163.3	137.9	175.4	145.4	121.2	120.6	131.7	111.6	142.6	123.0	125.0	129.9	116.3	160.7	116.3	129.9	–
3	163.3	131.9	163.1	150.8	120.9	120.3	131.2	111.6	142.1	122.8	125.6	129.0	116.2	159.7	116.2	129.0	–
4	163.2	131.9	163.1	147.8	120.9	120.2	131.1	111.6	142.2	122.8	126.1	115.8	151.9	150.8	110.1	122.3	64.4[a] 15.1[b]
5	163.2	131.9	163.1	150.9	120.9	120.3	131.0	111.6	142.4	123.0	112.3	121.9	111.4	128.6	120.6	151.8	–
6	163.2	131.9	163.2	149.4	120.9	120.3	131.1	111.6	143.3	123.0	126.1	109.0	150.9	151.8	115.7	122.4	55.9[c]
7	163.1	137.9	175.4	145.5	120.9	120.6	131.8	111.6	142.6	123.0	126.9	112.4	114.3	150.7	147.3	121.2	56.4[c]
8	163.2	138.1	163.1	142.9	122.9	120.9	131.9	111.4	142.3	124.9	131.2	104.9	148.7	151.8	148.7	104.9	56.6[c]
Calculated																	
1	169.2	137.7	156.6	151.9	126.5	128.5	137.4	115.9	148.9	127.7	141.6	137.4	134.8	136.3	135.0	129.6	–
2	168.7	138.2	182.0	156.2	127.1	128.6	138.2	116.1	149.6	127.6	132.4	140.6	119.7	167.6	120.7	132.6	–
3	169.0	137.7	156.5	151.8	126.4	128.5	137.3	115.8	148.8	128.1	133.2	139.3	119.6	166.8	120.6	131.6	–
4	168.7	137.2	156.4	153.0	126.0	128.3	137.4	115.6	148.3	127.2	133.6	118.1	153.2	155.9	119.4	122.5	69.0[a] 15.8[b]
5	169.2	137.7	156.0	154.4	126.4	128.5	137.6	115.9	149.0	127.1	123.8	137.6	124.2	137.9	121.5	167.4	–
6	168.7	138.1	156.5	152.4	126.2	128.4	137.4	115.8	148.5	128.0	133.3	117.4	153.5	156.3	119.4	122.3	57.6[c]
7	168.5	138.5	182.0	156.5	127.0	128.7	138.2	116.1	149.5	127.9	133.2	131.2	114.4	157.3	153.9	114.1	57.9[c]
8	168.9	137.8	156.6	152.0	126.6	128.5	137.3	115.9	148.7	128.2	132.6	125.6	153.8	150.2	155.4	105.8	63.5[c] 58.3[c]

Subs.: Substituents, a: CH_2, b: CH_3, c: OCH_3

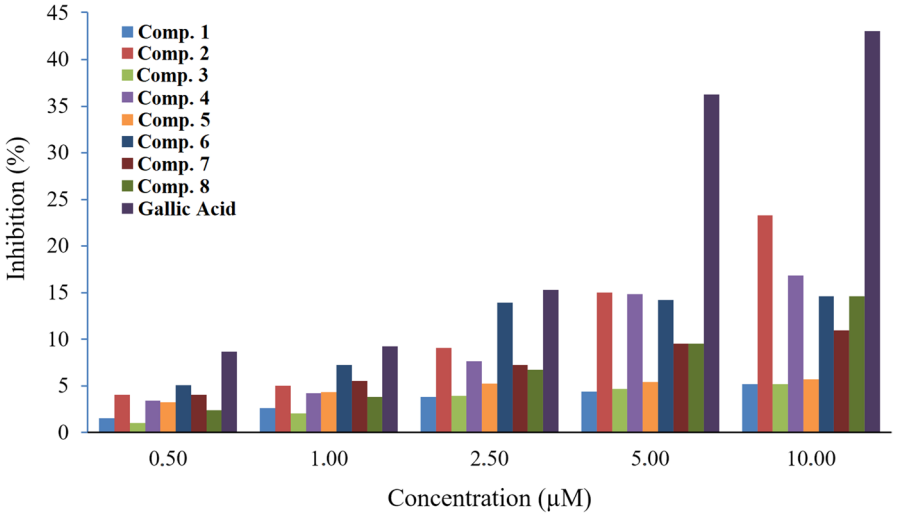

Fig. 4 Percentage change of inhibition calculated by DPPH method for gallic acid and compounds **1–8**

Table 6 IC_{50} values of the synthesized compounds

Comp	DPPH, RSA, IC_{50} (µM)*	R^2
1	54.13 ± 0.12	0.983
2	10.99 ± 0.03	0.923
3	45.55 ± 0.11	0.956
4	13.84 ± 0.04	0.932
5	77.95 ± 0.15	0.886
6	17.99 ± 0.06	0.835
7	26.96 ± 0.09	0.994
8	17.12 ± 0.06	0.958
Gallic acid	5.87 ± 0.01	0.890

*IC_{50} = concentration (µM) indicating inhibition of 50% DPPH radical. Values are expressed as mean (n = 3), RSA: radical scavenging activity

Table 7 Calculated electronic parameters of the compounds

Comp.	E (a.u)	E_{HOMO} (eV)	E_{LUMO} (eV)	ΔE (eV)	η	χ (eV)	α (a.u)
1	− 1042.035	− 6.283	− 2.757	3.526	1.763	4.520	283.2
2	− 1440.241	− 5.913	− 2.869	3.044	1.522	4.391	335.7
3	− 1117.286	− 5.975	− 2.712	3.263	1.631	4.343	292.7
4	− 1271.179	− 5.727	− 2.694	3.034	1.517	4.211	327.6
5	− 1117.296	− 6.107	− 2.866	3.241	1.620	4.487	289.9
6	− 1231.847	− 5.762	− 2.705	3.057	1.529	4.233	313.2
7	− 1554.802	− 5.820	− 2.821	2.998	1.499	4.321	359.0
8	− 1346.403	− 5.776	− 2.706	3.070	1.535	4.241	333.4

E: molecular energy,$\Delta E = E_{LUMO} - E_{HOMO}$, χ: electronegativity, η: chemical hardness, α: polarizability

properties. This result also revealed that the substituents have an active role in determining antioxidant properties. It was observed that among the compounds showing similar conformational and structural properties (compounds **2** and **3**), the sulfur-containing compound **2** has lower ΔE than the oxygen-containing compound **3** and showed more antioxidant effect. Compounds with smaller ΔE values in compounds **3** and **4** (3.263 eV and 3.034 eV, respectively) and compounds **4** and **6** (3.034 eV and 3.057 eV, respectively), which differ only in terms of *m*-substituents, also showed higher antioxidant properties. Chemically hard molecules show low polarizability (stable electron distributions), and the chemical hardness is related to the energy gap ΔE. At this point, it was seen that a similar relationship for the respective compounds was also between the chemical hardness of the compounds and hence their polarizability. HOMO–LUMO and ESP maps of compounds **2** and **3** are given in Fig. 5. (All the HOMO–LUMO and ESP maps of the compounds are given in supplementary material A.)

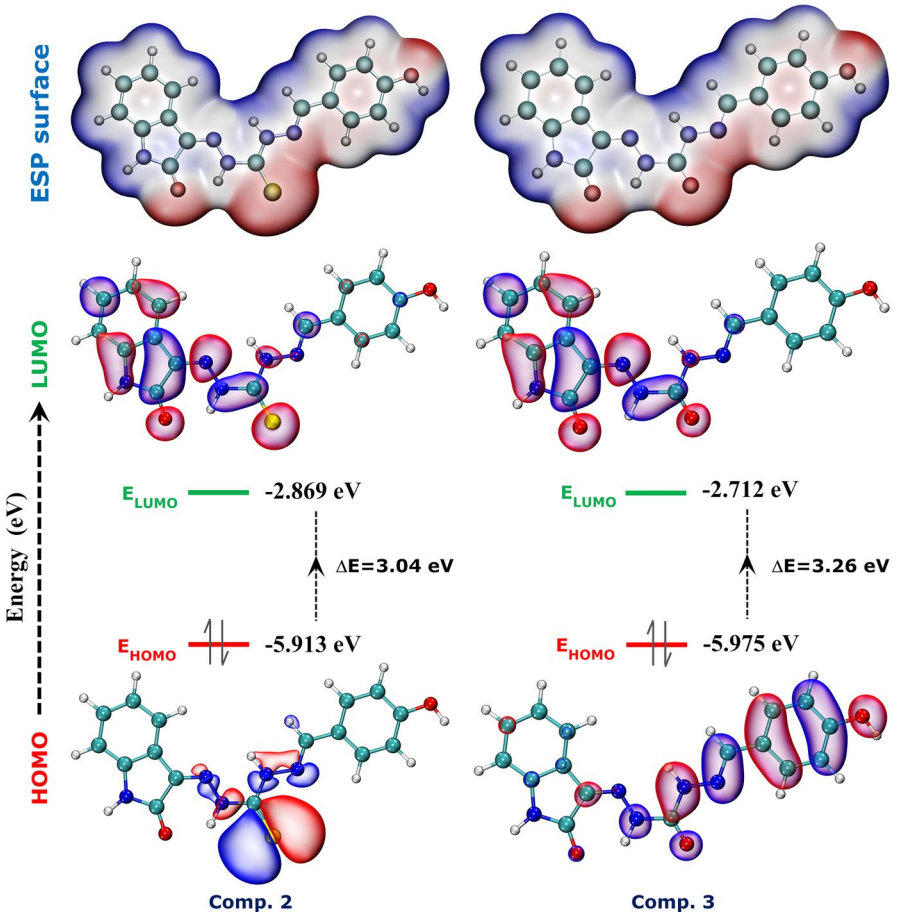

Fig. 5 HOMO–LUMO and ESP maps of compounds **2** and **3**

The phenolic O–H bond of compound **2** results from the overlap of a *s-p* hybrid on O with an *s* orbital on H. The phenolic O–H hybridization of compound **2** was calculated as $\sigma_{OH} = 0.8600\left(sp^{3.76}\right)_O + 0.5102(s)_H$. For compound **3**, it was calculated as $\sigma_{OH} = 0.8599\left(sp^{3.76}\right)_O + 0.5105(s)_H$. Although the hybridization on the phenolic oxygen atom was the same in both compounds, the polarization coefficient of the phenolic oxygen atom of compound **2** was calculated to be higher than that of compound **3** due to the effect of the sulfur. In addition, it was observed that the polarization coefficient of phenolic oxygen in *m*-substituted compounds was higher than that of compound **3** but the degree of *s-p* hybridization was lower ($\sigma_{OH} = 0.8656\left(sp^{3.63}\right)_O + 0.5007(s)_H$ for compound **4**, $\sigma_{OH} = 0.8656\left(sp^{3.63}\right)_O + 0.5008(s)_H$ for compound **6** and $\sigma_{OH} = 0.8671\left(sp^{3.59}\right)_O + 0.4982(s)_H$ for compound **8**).

Density of state (DOS) of a system is the proportion of states occupied by the system at each energy level. DOS data of compounds **2** and **3** are given in Fig. 6. Although HOMO–LUMO energies have an effect on the reaction characteristics of compounds, it was seen that the state densities of electrons in occupied orbitals also contribute to the reaction. In addition, it was calculated that the electron state density of low-energy HOMOs in sulfur-containing compound **2** was higher than that of compound **3**. In addition, when compared with the non-substituted compound **1**, it was observed that the substituents caused an increase in the electron density of state in the HOMOs of the compounds. All the DOS maps of the compounds are given in supplementary material B.

QTAIM, NCI and Fukui analysis of the compounds revealed more clearly the effects of substituents on the molecular structure and their contribution to the antioxidant characteristics. NCI calculations showed that (N2–H)–O and (N1–H)–N intramolecular interactions were strong and H1–N, (imine-H)–(N1–H) and (imine-H)–H5 interactions were weak. It was also observed that the imine group nitrogen atoms showed a strong intramolecular interaction with both the benzene ring and

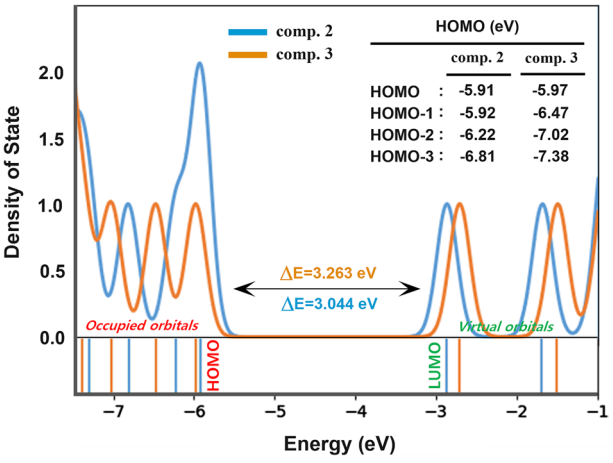

Fig. 6 Electron density of state (DOS) at the HOMO–LUMO energy level of compounds **2** and **3**

the sulfur or oxygen atoms (Fig. 7 and supplementary material C). Furthermore, Fukui calculations also revealed that the sulfur atom enhances electron localization through electronegative atom groups and also expands the electrophilic attack sites in the aryl region (Fig. 7).

Phenolic *p*-OH acts as an electron donor to the aromatic ring by p–π conjugation. *m*-Substituents withdraw electrons from the ring by inductive effect, but this one is weaker than the resonance effect of the *p*-OH substituent. QTAIM and NCI calculations revealed that the intramolecular interaction between *p*-OH and *m*-substituents reduces the electron density on the phenolic O–H bond. The inductive electron-withdrawing behavior of *m*-substituents caused a decrease in the electron density of the bond between the imine group and the benzene ring, at the benzene-RCP, and on the phenolic O–H bond, resulting in increased antioxidant activity compounds **4**, **6** and **8**. Electron density on the phenolic O–H bond was calculated as 0.374574 au for

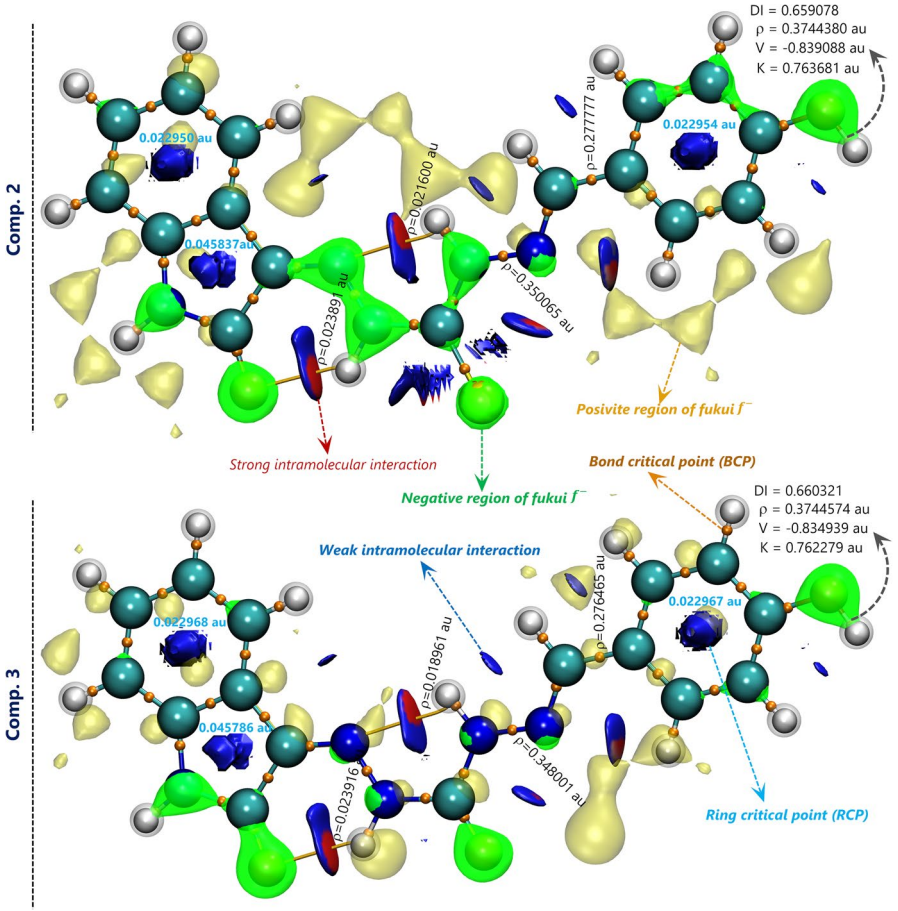

Fig. 7 QTAIM, NCI and Fukui maps of compounds **2** and **3** (ρ: electron charge density, **DI**: delocalization index, **V**: potential energy density, **K**: kinetic energy density)

compound **3**, while it was calculated as 0.369774 au, 0.369876 au and 0.368506 au for compounds **4**, **6** and **8**, respectively (supplementary material C). Bond strength is proportional to the electron density on the bond. The intramolecular interaction of *m*-substituents with phenolic O–H reduced the O–H bond strength and enhanced the antioxidant behavior of the related compound.

Oxygen is more electronegative than sulfur and bonds to oxygen are more polar than corresponding bonds to sulfur, and also the electron affinity of oxygen is smaller than that of sulfur, and as a consequence, sulfur allows more freedom of electron localization in the aryl region than oxygen. In compound **2**, the electron density between the phenol ring and the imine group (0.277777 au) is larger than that of compound **3** (0.2776465 au) and smaller than that of compound **3** at the RCP of the benzene ring (0.022954 au for compound **2** and 0.022967 au for compound **3**). When these data are compared with that of compound **1**, the effect of both phenolic –OH and sulfur atom on electron localization is seen more clearly (see supplementary C).

Delocalization of electrons has an effect on increasing the stability of the system compared to the localized states, and the calculations predict that the DI value of compound **2** (0.659078) is lower than that of compound **3** (0.660321), and as a result, it exhibits higher antioxidant properties than compound **3**, in agreement with the experimental results.

The electron delocalization index (DI) between phenolic oxygen and hydrogen atoms (O–H), which play an active role in the DPPH reactions of the compounds, was also affected by *m*-substituents. The delocalization indices of *m*-substituted compounds **4**, **6** and **8** are lower than that of compound **3**, but their antioxidant properties are higher (see supplementary C). Similar relationships were observed for the kinetic energy and potential energy densities of the phenolic OH bond. Moreover, it was calculated that the *m*-substituents in compounds **4**, **6** and **8** increased the bond path length (1.774903 Å, 1.774686 Å and 1.776110 Å, respectively) and bond length (0.96552 Å, 0.96541 Å and 0.96625 Å, respectively) of the phenolic O–H compared to compound **3** (1.769129 Å for BPL and 0.96188 Å for BL), which also increased the antioxidant properties of the compounds.

Conclusions

A series of new isatin-based Schiff base derivatives were prepared from (thio)/carbohydrazide and various aromatic aldehydes. The structure of all the products was elucidated by using IR, ^{1}H NMR and ^{13}C NMR spectroscopic methods and elemental analyses. The in vitro antioxidant activity of the molecules was tested by the DPPH free radical trapping process. IC_{50} values of the obtained products ranged from 10.99 ± 0.03 to 77.95 ± 0.15 μM. The antioxidant activities differed according to the structures of the aldehyde groups forming the Schiff bases and the type of the reactivity enhancing atom (O or S) attached to the carbohydrazone groups.

DFT calculations that validate experimental data showed that compounds with smaller ΔE values showed higher antioxidant properties and a similar relationship was found between the chemical hardness and polarizability of the compounds. In

addition, the relationship between the state densities of the electrons in the occupied orbitals and the antioxidant properties of the compounds was revealed. The effect of sulfur atom with low electron affinity to electron distribution on the molecule was demonstrated, and electrophilic attack sites were visualized using NCI and Fukui maps. The calculations revealed that the electron density of phenolic O–H bond at BCP, as well as kinetic energy and potential energy density and electron delocalization on the bond, could be useful tools for comparing and predicting the antioxidant properties of compounds.

Supplementary materials

IR, ^{1}H NMR and ^{13}C NMR spectra of the compounds and the QTAIM, NCI, Fukui, HOMO–LUMO and ESP maps are given in supporting information.

Supplementary Information The online version contains supplementary material available at https://doi.org/10.1007/s11164-021-04576-7.

Author contributions Halit Muğlu was involved in synthesis, methodology and structure elucidation. Hasan Yakan was involved in synthesis, structure elucidation and writing—original draft preparation. Amhimmid Ghayth Amhimmid Misbah contributed to synthesis and methodology. M. Serdar Çavuş was involved in density functional theory calculations and writing—original draft preparation. Temel Kan Bakır was involved in antioxidant activity studies and writing—original draft preparation.

Declarations

Conflict of interest The authors declare that they have no conflict of interest. Also, synthesis, structure elucidation and antioxidant activity parts of this study belong to Amhimmid G. A. Misbah master thesis at Kastamonu University.

References

1. S.N. Pandeya, S. Smitha, M. Jyoti, S.K. Sridhar, Acta. Pharm. **55**, 27 (2005)
2. H. Muğlu, H. Yakan, T.K. Bakır, Turk. J. Chem. **44**, 237 (2020)
3. H. Muğlu, Res. Chem. Intermed. **46**, 2083 (2020)
4. A. Jarrahpour, D. Khalili, E. De Clercq, C. Salmi, J. Brunel, Molecules **12**, 1720 (2007)
5. D. Sriram, T.R. Bal, P. Yogeeswari, Med. Chem. Res. **14**, 211 (2005)
6. R. Cheng, X. Yan, Z. Xu, J. Heterocycl. Chem. **56**, 2970 (2019)
7. K. Meenakshi, N. Gopal, M. Sarangapani, Int. J. Pharm. Pharm. Sci. **6**, 318 (2014)
8. A.V. Bogdanov, I.F. Zaripova, A.D. Voloshina, A.S. Sapunova, N.V. Kulik, S.V. Bukharov, J.K. Voronina, A.E. Vandyukov, V.F. Mironov, ChemistrySelect **4**, 6162 (2019)
9. S.Y. Abbas, A.A. Farag, Y.A. Ammar, A.A. Atrees, A.F. Mohamed, A.A. El-Henawy, Monatsh. Chem. **144**, 1725 (2013)
10. T.R. Bal, B. Anand, P. Yogeeswari, D. Sriram, Bioorg. Med. Chem. Lett. **15**, 4451 (2005)
11. S.K. Sridhar, S.N. Pandeya, J.P. Stables, A. Ramesh, Eur. J. Pharm. Sci. **16**, 129 (2002)
12. T. Aboul-Fadl, F.A. Bin-Jubair, Int. J. Res. Pharm. Sci. **1**, 113 (2010)
13. R. Sabet, M. Mohammadpour, A. Sadeghi, A. Fassihi, Eur. J. Med. Chem. **45**, 1113 (2010)
14. N. Deswal, A. Shrivastava, M. Summon Hossain, P. Gahlyan, R. Bawa, R.D. Gupta, R. Kumar, ChemistrySelect **6**, 717 (2021)
15. Q.P. Diao, H. Guo, G.Q. Wang, J. Heterocycl. Chem. **56**, 1687 (2019)
16. L. Pogány, J. Moncol, J. Pavlik, M. Mazúr and I. Šalitroš ChemPlusChem **84**, 358 (2019)

17. S. Shukla, R. Srivastava, S. Shrivastava, A. Sodhi, P. Kumar, Med. Chem. Res. **22**, 1604 (2013)
18. F. Rahim, F. Malik, H. Ullah, A. Wadood, F. Khan, M.T. Javid, M. Taha, W. Rehman, A.U. Rehman, K.M. Khan, Bioorg. Chem. **60**, 42 (2015)
19. D.P. Shelar, T.-T. Li, Y. Chen, W.-F. Fu, ChemPlusChem **80**, 1541 (2015)
20. S.S. Ali, E.-R. Kenawy, F.I. Sonbol, J. Sun, M. Al-Etewy, A. Ali, L. Huizi, N.A. El-Zawawy, Pharm. Res. **36**, 5 (2019)
21. A. Cinarli, D. Gürbüz, A. Tavman, A.S. Birteksöz, Bull. Chem. Soc. Ethiop. **25**, 407 (2011)
22. T.K. Bakır, J.B. Lawag, Res. Chem. Intermed. **46**, 2541 (2020)
23. S. Shamim, S. Murtaza, M.F. Nazar, J. Chem. Soc. Pak. **38**, 494 (2016)
24. H. Yakan, T.K. Bakır, M.S. Çavuş, H. Muğlu, Res. Chem. Intermed. **46**, 5417 (2020)
25. A.S. Hassan, T.S. Hafez, S.A.M. Osman, M.M. Ali, Turk. J. Chem. **39**, 1102 (2015)
26. E. Hejchman, H. Kruszewska, D. Maciejewska, B. Sowirka-Taciak, M. Tomczyk, A. Sztokfisz-Ignasiak, J. Jankowski, I. Młynarczuk-Biały, Monatsh. Chem. **150**, 255 (2019)
27. A. Saeed, R. Qamar, T.A. Fattah, U. Flörke, M.F. Erben, Res. Chem. Intermed. **43**, 3053 (2017)
28. H. Yakan, M.S. Çavuş, B.Z. Kurt, H. Muğlu, F. Sönmez, E. Güzel, J. Mol. Struct. **1239**, 130495 (2021)
29. A.A. Al-Amiery, Y.K. Al-Majedy, H.H. Ibrahim, A.A. Al-Tamimi, Org. Med. Chem. Lett. **2**, 4 (2012)
30. D.-P. Yang, H.-F. Ji, G.-Y. Tang, W. Ren, H.-Y. Zhang, Molecules **12**, 878 (2007)
31. S.J. Berners-Price, J. Biol. Inorg. Chem. **12**, S7 (2007)
32. G. Kiran, M. Sarangapani, T. Gouthami, A.R. Narsimha Reddy, Toxicol. Environ. Chem. **95**, 367 (2013)
33. A. Andreani, S. Burnelli, M. Granaiola, A. Leoni, A. Locatelli, R. Morigi, M. Rambaldi, L. Varoli, M.A. Cremonini, G. Placucci, Eur. J. Med. Chem. **45**, 1374 (2010)
34. K.M. Khan, M. Khan, N. Ambreen, F. Rahim, B. Muhammad, S. Ali, S.M. Haider, S. Perveen, M. Choudhary, J. Pharm. Res **4**, 3402 (2011)
35. M. Premanathan, S. Radhakrishnan, K. Kulangiappar, G. Singaravelu, V. Thirumalaiarasu, T. Sivakumar, K. Kathiresan, Indian J. Med. Res. **136**, 822 (2012)
36. G. Kiran, T. Maneshwar, Y. Rajeshwar, M. Sarangapani, J. Chem. **2013**, 192039 (2012)
37. D. Kumar, D.S. Rawat, Bioorg. Med. Chem. Lett. **23**, 641 (2013)
38. W. Brand-Williams, M.-E. Cuvelier, C. Berset, LWT-Food Sci. Technol. **28**, 25 (1995)
39. H. Yaşa, Turk. J. Chem. **42**, 1105 (2018)
40. N. Naik, H. Vijay Kumar, P.B. Vidyashree, J. Pharm. Res. **4**, 2686 (2011)
41. E.N. Frankel, A.S. Meyer, J. Sci. Food Agric. **80**, 1925 (2000)
42. M. Frisch, G. Trucks, H. Schlegel, G. Scuseria, M. Robb, J. Cheeseman, G. Scalmani, V. Barone, B. Mennucci, G. Petersson, D. Fox, Gaussian 09 C01. Gaussian Inc, (Wallingford, CT, 2010)
43. W. Kohn, L.J. Sham, Phys. Rev. **140**, A1133 (1965)
44. P. Hohenberg, W. Kohn, Phys. Rev. **136**, B864 (1964)
45. A.E. Reed, L.A. Curtiss, F. Weinhold, Chem. Rev. **88**, 899 (1988)
46. J. Carpenter, F. Weinhold, J. Mol. Struct. THEOCHEM **169**, 41 (1988)
47. A.E. Reed, R.B. Weinstock, F. Weinhold, J. Chem. Phys. **83**, 735 (1985)
48. A.E. Reed, F. Weinhold, J. Chem. Phys. **83**, 1736 (1985)
49. A.E. Reed, F. Weinhold, J. Chem. Phys. **78**, 4066 (1983)
50. D. Dimić, M. Petković, Int. J. Quantum Chem **116**, 27 (2016)
51. R.F. Bader, Chem. Rev. **91**, 893 (1991)
52. M. Izadyar, M. Khavani, Int. J. Quantum Chem **114**, 666 (2014)
53. R.F. Bader, Acc. Chem. Res. **18**, 9 (1985)
54. W. Nakanishi, S. Hayashi, T. Nishide, S. Otsuki, Int. J. Quantum Chem **120**, e26073 (2020)
55. O. Bekircan, H. Bektas, Molecules **13**, 2126 (2008)
56. D. Williams, I. Fleming, RNA structure and NMR spectroscopy. Spectroscopic Methods in Organic Chemistry, (McGraw-Hill, New York, 1996)
57. M.S. Çavuş, H. Yakan, H. Muğlu, T. Bakır, J. Phys. Chem. Solids **140**, 109362 (2020)
58. H. Muğlu, M.S. Çavuş, T. Bakır, H. Yakan, J. Mol. Struct. **1196**, 819 (2019)

Authors and Affiliations

Halit Muğlu[1] · Hasan Yakan[2] · Amhimmid Ghayth Amhimmid Misbah[1] · M. Serdar Çavuş[3] · Temel Kan Bakır[1]

✉ Hasan Yakan
hasany@omu.edu.tr

✉ M. Serdar Çavuş
mserdarcavus@kastamonu.edu.tr

[1] Department of Chemistry, Faculty of Art and Science, Kastamonu University, Kastamonu, Turkey

[2] Department of Mathematics and Science Education, Faculty of Education, Ondokuz Mayis University, Samsun, Turkey

[3] Biomedical Engineering Department, Faculty of Engineering and Architecture, Kastamonu University, Kastamonu, Turkey